AAPG Annual Meeting
March 10-13, 2002
Houston, Texas

Estimation of Net-to-Gross from P and S Impedance: Integration of Petrophysics and 3D Seismic Inversion

Vernik, Lev, Bp, Houston, Tx; David Fisher, Bp, Houston, Tx; Steve Bahret, Jason Geosystems, Houston, Tx

Summary

Estimation of net-to-gross (N/G) on a field wide scale was accomplished by integrating rock property trends and high quality 3D seismic data. Edited and anisotropy-corrected sonic logs from deepwater Gulf of Mexico (GoM) were used in combination with core velocity measurements and Biot-Gassmann modeling to determine shale and oil sand trends in low-frequency Vp-Vs space. These trends equally apply in the acoustic impedance (AI) and shear impedance (SI) crossplot. Shale and oil saturated sand trends in the Horn Mountain field, deepwater GoM, are basically parallel in the AI-SI crossplot and effectively bracket the reservoir facies distribution. Accurate estimates of sand volume fraction (1-Vsh) are obtainable from a simple linear interpolation between the AI-SI trends. Four angle range stacks from a 3D survey over the field were calibrated and constrained by available well control and simultaneously inverted to AI and SI. The impedance volumes closely match the upscaled log data and were combined using linear interpolation between the sand and shale trends to create a sand fraction volume. Integration of the sand fraction over the gross reservoir thickness provides an estimate of N/G at any x-y location. N/G maps can be used to predict net-to-gross, predominant lithofacies and net sand thickness away from well control. The quantitative results obtained using N/G mapping markedly enhanced reservoir description of the Horn Mountain field.

Introduction

Net-to-gross evaluation is often a key issue in reservoir characterization projects. Here, we are concerned with the Horn Mountain field, deepwater GoM, where reservoirs in the field are friable sands originally deposited in a deepwater turbidite channel/levee system. The Horn Mountain log model, including petrofacies classification, was developed without any input from sonic logs. Therefore, a special effort was required to marry it to the high quality 3D seismic data set. Notably, we have sought confirmation of the petrofacies classification and ability to compute shale volume fraction merely from Vp-Vs or AI-SI crossplots.

Anisotropy modeling

Mismatch between the log Vp and Vs values in deviated wells and those in shale-dominated intervals in the straight holes prompted velocity anisotropy measurements on core samples. Anisotropic effective media modeling was carried out in order to understand the effective properties of the ubiquivitous levee facies composed of laminated sand (silt) and shale. The best fit anisotropy model as a function of laminar Vsh was developed, where anisotropy parameters were computed from the effective elastic constants, and applied to sonic logs run in deviated wells. The significance of the anisotropy correction and its dependence on Vsh can be visualized in Figure 1, which is a log plot of the M zone in one of the deviated wells with relative dip about 63°.

Vp-Vs relationships and the AI-SI crossplot

Since an empirically substantiated, theoretical relationship between Vp and Vs can only be invoked for sandstones with porosities below the consolidation porosity (24 to 29%), we proceed mostly along empirical lines in an attempt to explore the Vp^2-Vs^2 space in terms of major petrofacies distinguished in the log model for Horn Mountain. In an expanded paper (Vernik and Fisher, 2001), we show that the equation that best fits BP GoM log and core database for both 'hard' and 'soft' sands is:

$$Vs = (a + bVp^2 + cVp^4)^{0.5} \quad (R=0.963) \qquad (1)$$

a = - 1.267; b = 0.372; c = 2.84e-03.

We also show that the log shale trend is very consistent with the core shale data and, in the wide range of Vp from 2.7 to 4.5 km/s, can be accurately described by the RMA model:

$$Vs = 0.70Vp - 0.67 \qquad (R=0.946). \qquad (2)$$

Using brine-to-oil fluid substitution on equation (1), we arrive at a quasi-linear trend showing excellent agreement with the Horn Mountain oil sand data. The most important realization of this data-driven modeling is that over the velocity range of interest in this study the slope of the oil sand quasi-linear trend is very close to 0.7, i.e., it is practically the same as the slope of the shale equation (2).

The petrophysical classification of the Horn Mountain reservoir was achieved by combination of core- and log model-derived physical properties, such as Vsh, porosity, permeability, and fluid saturation. To marry the log model petrofacies classification to the 3D seismic inversion it is imperative to demonstrate that the major petrophysical groups can also be distinguished on the AI-SI crossplot. A crossplot utilizing only data above the OWC with color-coded petrofacies is shown in Figure 2. It is noteworthy, that each petrofacies finds its own place in AI-SI space, providing independent confirmation for the log model classification. The parallel trends (of slope 0.7) for shale and oil sand end member petrofacies can be used for linear interpolation resulting in sand volume

fraction estimation. Integrating the latter over the gross reservoir thickness results in the total N/G estimate for each well showing remarkable agreement with log model N/G values.

Seismic Inversion

The 3D seismic data at Horn Mountain were prestack time migrated and provided a high quality set of flat gathers. Based on amplitude, frequency, and continuity segregation, the data were separated into four angle ranges prior to stacking: 0-22°, 20-45°, 30-55° and 40-65°. As shown in Figure 3, the angle range stacks show significant variations in amplitude typically associated with Vp/Vs contrast between blocky oil sand and shale that is indirectly related to the oil sand thickness and quality.

Inputs to simultaneous inversion were four seismic angle stacks, the corresponding seismic wavelets, and several constraining relationships. The simultaneous inversion process generates volumes of AI, SI, and density. AI is primarily a function of the near angle stack while SI reconstructs the best overall fit to observed reflectivity changes across the seismic volumes.

As shown in Figure 2, the anisotropy corrected dipole shear log data show distinct grouping of petrophysical facies in AI-SI space. Upscaling the log impedances to match seismic vertical resolution by simple smoothing (Figure 4) results in the expected shrinkage of data cloud on the crossplot, similar to the transition from log to seismic inversion data shown in Figures 2a and 2b, respectively. However, for either data set, the position of the shale-dominated sections with respect to the log-derived, normal compaction (or slightly overpressured) shale trend with the slope of 0.7 remains basically unchanged. Again, in our case, the shale and oil sand trends are basically parallel and effectively bracket the reservoir facies distribution including levee deposits with variable sand volume fraction (1-Vsh). Linear interpolation of these end member trends results in equation (3):

$$Vsand = \frac{SI - bAI - a_0}{a_1 - a_0}, \qquad (3)$$

where *AI* and *SI* are the p and s impedances, respectively, *b* is the average slope of the shale b_o and hydrocarbon sand b_1 trends, and a_o and a_1 are their respective intercepts. In our case, a_o = -5360 and a_1 = -2740 g/cm^3*ft/s, and b = 0.7.

Results and Interpretation

Equation (3) with specified parameters was applied to the seismic inversion data generating a Vsand volume. 1D extractions from this volume at well locations are in excellent agreement with those computed using the same equation with upscaled AI and SI log inputs (Figure 4). The top and base time surfaces for both M and J reservoirs were intersected with the Vsand volume to extract the thickness-average

N/G. Figure 5a is the map showing this thickness-average N/G for the M2 interval. Next, the gross reservoir time interval was converted to depth thickness using anisotropy corrected well log velocities. The gross isochore was multiplied by the average N/G to compute the net oil sand thickness shown in Figure 5b. These maps derived from the AI and SI inversion data are vastly superior to those generated from a single AI inversion or single seismic amplitude extraction. The maximum offset amplitude response is honored in these inversions, exploiting the contrast in Vp/Vs found in the Horn Mountain field between channel sands, levees, and shale.

Figure 6, which plots our 3D seismic-based average N/G against the well average N/G for two reservoir zones, is an ultimate confirmation of the proposed technique at Horn Mountain. The accuracy of the prediction is within 0.10. The RMA regression slope for the M2 zone is close to 45° and the only outlier (well #7) is due to poor seismic quality in the vicinity of a salt dome. This quality control check contains reservoir zones from six development wells that were not available when the inversion and AI-SI analysis was carried out.

Based on the core data, the areas of N/G greater than 0.6 (hot colors on the map) are interpreted to be largely made of channel sands with darcy range permeability, while areas of low N/G from 0.2 to 0.5 are dominated by thin sand and laminated levee deposits with permeability in the 100 to 400 mD range. The orientation of the high permeability channel fairways can be seen in the N/G map oriented from the NW to SE. N/G values below 0.1 can be deemed nonpay. Obviously, coefficients in the impedance to N/G transform given by equation (3) should be re-adjusted below the OWC, if we are to map sand thickness in the aquifer.

Conclusions

Using edited and anisotropy-corrected sonic logs from deepwater GoM in combination with published core velocity measurements and Biot-Gassmann modeling, we refine major trends in low-frequency Vp-Vs space and extend them to the AI-SI crossplot. Vsand curves computed using linear interpolation between the end member sand and shale trends are integrated over the gross reservoir thickness to produce log model-consistent estimates of N/G in each appraisal well. Simultaneous inversion for AI and SI is quite robust and closely matches the anisotropy corrected log data. The impedance volumes were combined using the same linear interpolation between the sand and shale trends to create a sand fraction volume from which N/G maps are extracted. The quantitative results obtained using N/G mapping markedly enhanced reservoir description of the Horn Mountain field and the subsurface team is currently using these data for detailed reservoir description and field development planning.

References

Vernik, L. and Fisher, D., 2001, Estimation of net-to-gross from P and S impedance: Part I – petrophysics: 71st Ann. Int. SEG Mtg, Expanded Abstracts.

Acknowledgement

All seismic data utilized in this paper is owned by TGS, CGG, and Western GECO. The authors thank BP management for permission to publish this work.

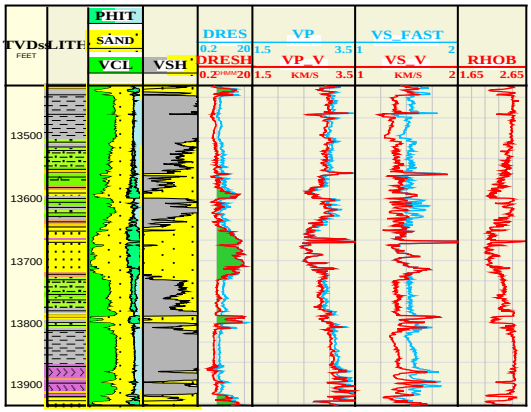

Figure 1: Log plot of M-zone in a deviated well showing anisotropy correction carried out for deep resistivity, Vp, and Vs logs.

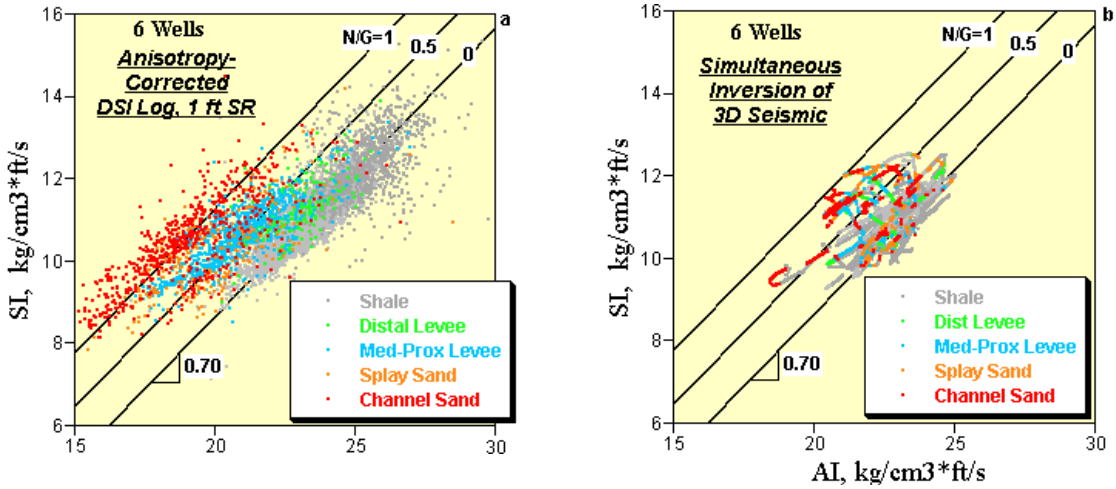

Figure 2: Crossplot of AI and SI from logs (a) and simultaneous inversion (b) showing major petrophysical facies and N/G trends.

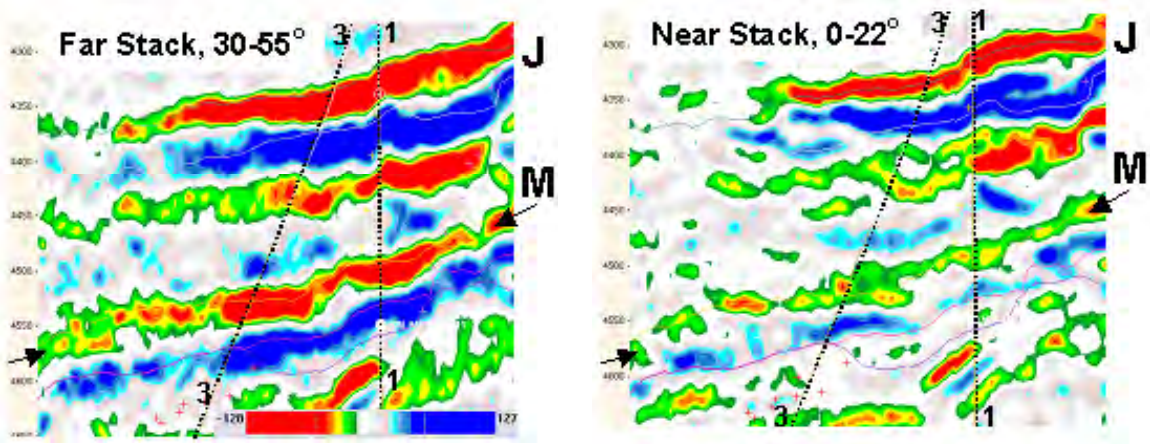

Figure 3: Seismic section through the near and far angle stack volumes. This section runs NW to SE through wells #1 and #3.

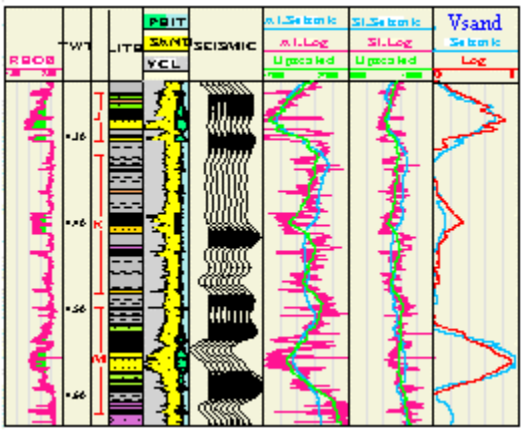

Figure 4: Log plot of AI, SI, and Vsand computed from upscaled logs and simultaneous inversion of 3D seismic.

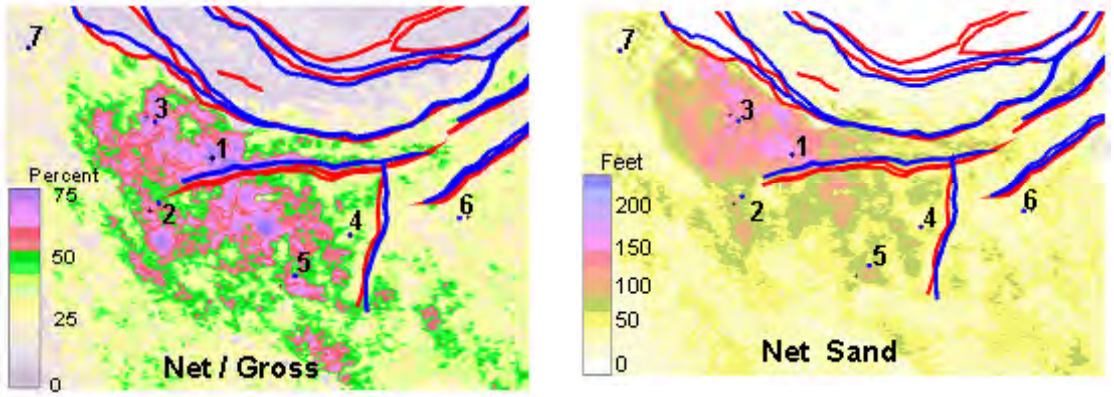

Figure 5: Thickness average N/G map and net oil sand feet map for the M2 interval.

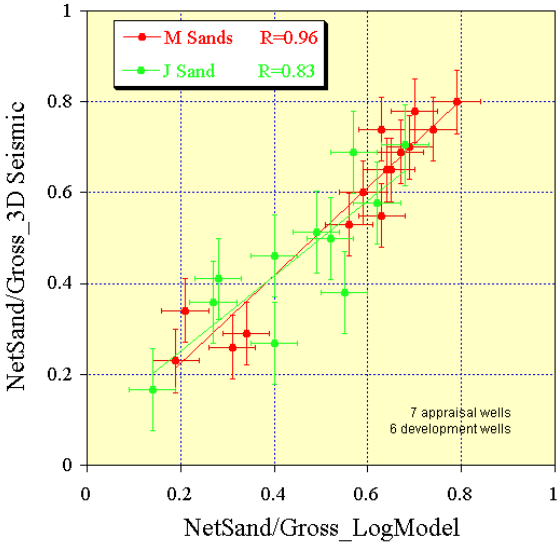

Figure 6: Well average N/G values from log model and 3D seismic inversion.